

# Fluorescence quantum yield of Yb<sup>3+</sup>-doped tellurite glasses determined by thermal lens spectroscopy

S.M. Lima <sup>a</sup>, A.K.R. Souza <sup>a</sup>, A.P. Langaro <sup>a</sup>, J.R. Silva <sup>a</sup>, F.B. Costa <sup>a, b</sup>, J.C.S. Moraes <sup>b</sup>,  
M.S. Figueiredo <sup>c</sup>, F.A. Santos <sup>c</sup>, M.L. Baesso <sup>d</sup>, L.A.O. Nunes <sup>e</sup>, L.H.C. Andrade <sup>a, \*</sup>

<sup>a</sup> Grupo de Espectroscopia Óptica e Fototérmica, Programa de Pós-Graduação em Recursos Naturais, Universidade Estadual de Mato Grosso do Sul, CP 351, Dourados, MS, Brazil

<sup>b</sup> Universidade Estadual Paulista, Departamento de Física e Química, Av. Brasil, 56, 15385-000, Ilha Solteira, SP, Brazil

<sup>c</sup> Universidade Federal da Grande Dourados, Faculdade de Ciências Exatas e Tecnologias, Dourados, MS, Brazil

<sup>d</sup> Departamento de Física, Universidade Estadual de Maringá, Av. Colombo 5790, 87020-900, Maringá, PR, Brazil

<sup>e</sup> Instituto de Física de São Carlos, Universidade de São Paulo, CP 369, 13560-970, São Carlos, SP, Brazil

## ARTICLE INFO

### Article history:

Received 15 June 2016

Accepted 29 August 2016

Available online 28 September 2016

### Keywords:

Fluorescence quantum yield  
Ytterbium doped tellurite glasses  
Optical spectroscopy  
Thermal lens spectroscopy

## ABSTRACT

In this work, the combination of three different thermal lens spectroscopic methodologies was used to better determine the fluorescence quantum yield and to observe the concentration quenching in Yb<sup>3+</sup>-doped binary tellurite glasses (in mol%, 80TeO<sub>2</sub> – 20Li<sub>2</sub>O and 80TeO<sub>2</sub> – 20WO<sub>3</sub>). The samples were synthesized by the conventional melt-quenching method and then studied using optical spectroscopy and thermal lens spectroscopy (TLS). These characterizations enabled investigation of the radiative and nonradiative processes involved in the ytterbium doped systems. High fluorescence quantum yield was obtained for low Yb<sup>3+</sup> doping (>90%), and in both glasses the Yb<sup>3+</sup> presented concentration quenching mainly caused by impurities, host-ion interaction and OH<sup>-</sup> vibrations. The observations suggested that there is a possibility of doping the glasses with higher Yb concentration (>1.6 × 10<sup>21</sup> ions/cm<sup>3</sup>) with low reduction of the quantum yield.

© 2016 Elsevier B.V. All rights reserved.

## 1. Introduction

The energy transfer from a sensitizer ion (rare-earth or transition metal) to an activator has been investigated aiming minimizing losses and the increase in efficiency of energy conversion in solar cells [1]. The high energy photons (UV–Vis) absorbed by the sensitizer are converted to photons of low energy by means of the downconversion (DC) mechanism. In this process the absorbed visible photon by the activator can generate two photons in the infrared spectral region. After the first publication of DC with Yb<sup>3+</sup> as activator [2], this phenomenon has been extensively investigated due to its radiative <sup>2</sup>F<sub>5/2</sub> → <sup>2</sup>F<sub>7/2</sub> transition that overlap with the energy band gap of silicon semiconductors. Depending on the structural characteristics of the host, the Yb<sup>3+</sup> spectroscopic properties can change significantly, which turns important investigating it before proposing the use as activator [3].

Yb<sup>3+</sup> ion can exhibit high fluorescence quantum yield ( $\eta$ ) when

inserted in hosts with reduced impurity levels (structural defects, OH<sup>-</sup>, etc) [4], so that the precise determination of  $\eta$  is very important for application in solar cell. Recently our group has investigated the optical and thermo-optical properties of different rare-earth doped tellurite glasses in order to consider them as host for activator and sensitizer ions [5–8]. Compared to other glasses, this kind of matrix presents advantageous on optical properties such as high linear and nonlinear refractive indices, low phonon energy, wide optical window transparency range, and higher rare earth solubility [9]. These glasses show good thermal and chemical stability, as well as a low melting point temperature [10]. These characteristics suggest tellurite system to be used in solar cell for matching the solar emission spectrum to the semiconductor cell. In fact, its high refractive index can contribute to minimize the energy loss due to the light reflection in the glass-solar cell interface. Other marks are that it is not hygroscopic, it is easy to synthesize, and depending on the sample composition, the phonon energy can be reduced significantly without changing much its refractive index. For practical application, tellurite glasses are promising because they exhibit some facilities to be deposited as film in

\* Corresponding author.

E-mail address: [luishca@uems.br](mailto:luishca@uems.br) (L.H.C. Andrade).

semiconductor cell [11].

The fluorescence quantum yield is one of the most important optical parameter of the luminescent ions, which measures the conversion of absorbed photons into emitted photons. Owing to its relevance, independently of the optical device, it has been determined by different methods, as integrating sphere [12], laser-induced optoacoustic spectroscopy [13], calorimetry [14], photoacoustic [15], thermal lens spectroscopy [16] and others. Each method has its own restriction for better determination of  $\eta$ , so that an absolute value with minimum error is often difficult.

In some  $\text{Yb}^{3+}$ -doped systems,  $\eta$  has been determined by the relation between the experimental and radiative lifetimes. In this case the main difficulty is the measurement of a correct  $\text{Yb}^{3+}$  lifetime due to the energy trapping effect [17]. This situation, for example, can be avoided by using Photothermal methods, where the sample is excited with a laser beam and, after absorption of the photon energy, measurement of the dynamic process of the fraction of absorbed energy converted into heat ( $\phi$ ) in the sample is performed. In other words, the non-radiative transitions are measured and related to the radiative ones. The evaluation of the fraction of radiative and nonradiative processes in fluorescent materials has shown to be an advantageous alternative route to determine  $\eta$ .

Among the photothermal methods, the thermal lens spectroscopy (TLS) is an effective technique that has been used for  $\eta$  determination in rare-earth doped materials as described by Baesso et al. in 1998 [16]. In this work, the concentration quenching of  $\text{Nd}^{3+}$ -doped low silica calcium aluminosilicate glass was measured and compared to theoretical  $\eta$  calculation. After that, Lima et al. [18] applied TLS in  $\text{Nd}^{3+}$ -doped ZBLAN glass by using multiwavelengths for excitation of the samples, so that no reference sample (undoped) is required, as firstly proposed by Baesso et al. Lastly, Jacinto et al. [19] combined the TLS with experimental lifetime data in order to also determine  $\eta$  for  $\text{Nd}^{3+}$ -doped phosphate, fluorozirconate and fluorindate glasses. This methodology proved to be very simple and does not require comparison with a reference sample or the use of multiple excitation wavelengths.

In this work, two sets of  $\text{Yb}^{3+}$ -doped tellurite glasses were synthesized and optically characterized. The  $\text{Yb}^{3+}$  fluorescence quantum efficiency was measured by using the TLS in different experimental configurations: with a reference sample, by using the multiwavelength form and the normalized lifetime thermal lens methodology. With this systematic study, a correct value for  $\eta$  is found, turning opportune a discussion on the  $\text{Yb}^{3+}$  concentration quenching in binary tellurite glasses.

## 2. Materials and methods

Binary tellurite glasses doped with ytterbium were prepared by the conventional melt-quenching method in the composition listed in Table 1. The reagents ( $\text{Li}_2\text{CO}_3$  99% purity VETEC;  $\text{TeO}_2 \geq 99\%$  and

$\text{Yb}_2\text{O}_3$  99.99% purity, Sigma-Aldrich) were weighed out, mixed in an agate mortar, and melted for 30 min in air in a platinum crucible at 850 °C for TL and 880 °C for TW glasses. The melt was poured into a stainless steel mold pre-heated near the glass transition temperature ( $T_g$ ). Subsequently, after thermal relaxation, the mold containing the glass was placed in a furnace for annealing in order to reduce the mechanical stress caused by thermal shock. The annealing was continued for 5 h at the same temperature ( $\sim T_g$ ), after that the glass was slowly cooled to room temperature. Finally, the produced glasses were cut and polished to different thicknesses in according to the demands of each experiment.

The sample densities ( $\rho$ ) were determined at room temperature by Archimedes' method, using distilled water as the immersion liquid. The energy dispersive spectroscopy (EDS) was realized using a scanning electron microscope (SEM), Carl Zeiss EVO LS-15, equipped with an Oxford Inca X-act detector (Oxford Instruments, Abingdon, Oxfordshire, UK). From  $\rho$  values, the calculated nominal ionic concentrations ( $N_{\text{calculated}}$ ) could be determined with an uncertainty  $\leq 5\%$ .

Ground state absorption spectra were obtained in the range of 300–1100 nm using a Cary 50 UV–Vis–NIR spectrophotometer. The near infrared emission intensities were measured by exciting at 920 nm with a Ti:sapphire laser pumped with a Verdi laser at 532 nm. The fluorescence signal was transmitted through an optical fiber to a spectrometer (Model MAYA 2000 Pro, Ocean Optics), which was previously calibrated in terms of its spectral response. Measurements of the  $^2\text{F}_{5/2}$  level luminescence lifetime were performed using a pulsed OPO laser (Surelite, Continuum SLI-10). In addition, Raman spectra were obtained by confocal microscopy BX51-Voyage, with 150 mW of laser excitation at 785 nm and resolution of  $3.0 \text{ cm}^{-1}$ .

The mode-mismatched dual-beam TLS configuration was used to measure  $\eta$  of the  $\text{Yb}^{3+}$ -doped tellurite glasses. In this setup, a tunable Ti:sapphire laser was used as the excitation source, and a HeNe laser at  $\lambda_p = 632.8 \text{ nm}$  was used as probe beam. Further details of the TLS experimental setup have been described previously [15,17,18].

## 3. Results and discussion

Fig. 1 shows the absorption coefficient ( $\alpha$ ) spectra in the UV–visible–NIR regions and the ytterbium emission spectra, with excitation at 920 nm, obtained for the 4.0 mol % of  $\text{Yb}^{3+}$ -doped TL and TW glasses. The inset shows the linear dependence of  $\alpha$  at 950 nm in function of the Yb amount determined by EDS technique (values listed as  $N_{\text{measured}}$  in Table 1). This linear behavior indicates a satisfactory incorporation of the ion into the glass, with Yb concentration higher into the TW matrix than TL one. Our assumption is that  $\text{Yb}_2\text{O}_3$  act as glass network modifiers more effectively in TW than TL host, creating a variety of dopant sites together with the

**Table 1**  
Nominal sample composition and Ytterbium concentration in mol%, volumetric density ( $\rho$ ), calculated and measured Yb concentration ( $N$ ), luminescence quantum efficiency determined by conventional ( $\eta_{\text{ref}}$ ), multiwavelength ( $\eta_{\text{multi}}$ ) and normalized lifetime ( $\eta_{\text{norm}}$ ) thermal lens methods. The uncertainty in  $\rho$ ,  $N_{\text{calculated}}$  and  $N_{\text{measured}}$  are 0.1%, 0.1% and 1%, respectively.

| Sample (mol%)                                      | $\text{Yb}_2\text{O}_3$ (mol%) | $\rho$ ( $\text{g}/\text{cm}^3$ ) | $N_{\text{calculated}}$ ( $10^{20}$ ions/ $\text{cm}^3$ ) | $N_{\text{measured}}$ ( $10^{20}$ ions/ $\text{cm}^3$ ) | $\eta_{\text{ref}}$ (%) | $\eta_{\text{multi}}$ (%) | $\eta_{\text{norm}}$ (%) |
|--|--------------------------------|-----------------------------------|---|---|-------------------------|---------------------------|--------------------------|
| 80% $\text{TeO}_2$ :20% $\text{Li}_2\text{O}$ (TL) | 0.5                            | 4.98                              | 2.2   | 1.8   | 98 $\pm$ 9              | 93 $\pm$ 9                | 90 $\pm$ 9               |
|  | 1.0                            | 5.01                              | 4.4   | 3.6   | 94 $\pm$ 9              | 81 $\pm$ 8                | 89 $\pm$ 9               |
|  | 2.0                            | 5.06                              | 8.8   | 7.4   | 88 $\pm$ 9              | 78 $\pm$ 8                | 81 $\pm$ 8               |
|  | 4.0                            | 5.18                              | 17.3  | 14.6  | 76 $\pm$ 8              | 66 $\pm$ 7                | 67 $\pm$ 7               |
| 80% $\text{TeO}_2$ :20% $\text{WO}_3$ (TW)         | 0.5                            | 5.97                              | 2.1   | 2.6   | 85 $\pm$ 9              | 96 $\pm$ 9                | 92 $\pm$ 9               |
|  | 1.0                            | 5.99                              | 4.1   | 4.5   | 80 $\pm$ 8              | 87 $\pm$ 9                | 89 $\pm$ 9               |
|  | 2.0                            | 6.03                              | 8.1   | 8.6   | 68 $\pm$ 7              | 76 $\pm$ 8                | 81 $\pm$ 8               |
|  | 4.0                            | 6.29                              | 16.6  | 15.7  | 61 $\pm$ 6              | 74 $\pm$ 7                | 68 $\pm$ 7               |

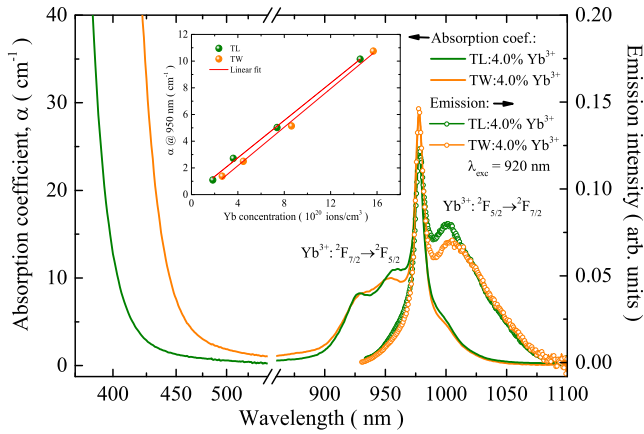


**Fig. 1.** Absorption coefficient and emission spectra for the 4.0 mol%  $\text{Yb}^{3+}$ -doped TL and TW glasses. The inset shows the Yb concentration dependence of the absorption coefficient at 950 nm for both TL and TW glasses.

glass formers. This is facilitated due the chemical proximity among Yb and W (atomic mass, electronegativity, etc). In this case, it can be expected that Yb can exhibit different electronic configuration in TW, so that in the total of ion concentration, the  $N_{\text{measured}}$  by EDS is higher in TW than TL host. Another important feature noted is that the Yb absorption and emission exhibit transitions between four stark manifolds of the  $^2\text{F}_{7/2}$  and three of  $^2\text{F}_{5/2}$  states, which depending on the glass host are not easy to be defined at room temperature.

A last interesting feature in Fig. 1 is the red shift noted to the fundamental absorption band in the UV region when TW is compared to TL glass. The observed reduction in the transparency window for TW glass is due to the influence of W atom into the crystalline field of the host, which is also responsible to an increase in the phonon energy of the host. Both the obtained Raman spectra for TW and TL glasses are plotted in Fig. 2. The  $\text{W-O}^-$  and  $\text{W=O}$  bonds of  $\text{WO}_4$  and  $\text{WO}_6$  units are observed around  $920\text{ cm}^{-1}$ , defining the phonon energy of TW glass [5], while for TL glass the phonon energy is around  $750\text{ cm}^{-1}$ , corresponding to the stretching vibrational mode of  $\text{Te-O}$  in the trigonal-pyramid units [20]. From the spectra it can be noted that the ratio of the intensities of absorptions associated to the  $\text{TeO}_4$  trigonal bipyramid units (at  $\sim 670\text{ cm}^{-1}$ ) and  $\text{TeO}_{3+1,3}$  trigonal pyramid units (at  $\sim 750\text{ cm}^{-1}$ ) is

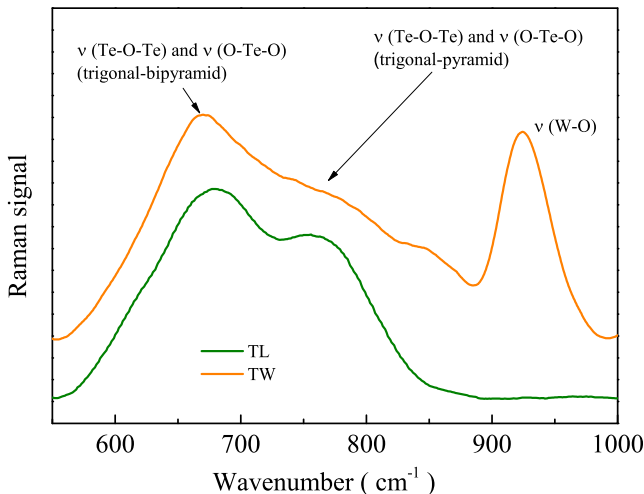


**Fig. 2.** Raman spectra for the TL and TW glasses.

higher in TW than TL glass, what is also related to the observed red shift in the fundamental absorption band.

By the emission spectra in Fig. 1, the average emission wavelength ( $\lambda_{\text{em}}$ ) = 1003 and 1004 nm were determined for TL and TW glasses, respectively. As it will be discussed later, this parameter is very important to calculate the fluorescence quantum yield ( $\eta$ ) by the TLS methodology. The emission spectra were also calculated by the reciprocity method [21,22] and a difference in the total emission area lower than 3% could be determined when compared to the experimental spectra. As expected for Yb ion, there is an overlap among the absorption and the emission spectra around the zero phonon line, which contributes to the Yb re-absorption mechanism (effect of radiation trapping). This fact turns difficulty to measure with precision the emission spectrum and to determine the  $\text{Yb}^{3+}$  lifetime.

In order to determine a precise  $\eta$  value for the Yb-doped tellurite sample sets, TLS was performed in different procedures: firstly,  $\eta$  was determined by using the conventional method in which a reference sample (undoped sample) is used to normalize the signal between the doped and undoped samples [16]; secondly, the TLS was applied in the multiwavelength form, in which no reference sample is required, and only the doped one is excited at different wavelengths in the ion absorption region [18]; after that, the TLS was combined with lifetime measurements to use the called normalized lifetime method [19]. The TLS methodology is based on a laser-induced thermal lensing effect in a partially transparent medium when the excitation laser beam passes through the sample and the absorbed energy is converted into heat, changing the optical path length,  $s$ , and producing a lens-like optical element in the sample. The propagation of the probe beam laser through the heated region will result in either a spreading ( $ds/dT < 0$ ) or a focusing ( $ds/dT > 0$ ) of the beam, depending mainly on the temperature coefficients of the thermal expansion and electronic polarizability of the sample. The theory described by Shen et al. [23] and that has been used in our study treats the thermal lens effect through the calculation of the temporal evolution of the sample temperature profile  $\Delta T(r, t)$ , caused by a Gaussian intensity distribution of the excitation beam.

To turn clearer the discussion, firstly it will be shown the results obtained using a reference sample. In this procedure, both undoped and Yb-doped tellurite sample sets were excited at 950 nm and the thermal lens signal was probed with a HeNe laser at 632.8 nm. Some values to the thermal lens signal,  $\theta$ , were obtained for different excitation powers,  $P$ , in order to find a better value to the ratio  $\theta/P$  for each sample. In the same sample position, the relation between the incident ( $P_0$ ) and transmitted ( $P$ ) power was measured to determine the absorption coefficient ( $\alpha$ ) with the well-known Beer's law relation:  $P = P_0(1 - R)^2 \exp(-\alpha L)$ , in which  $L$  is the sample thickness,  $R = [(n - 1)/(n + 1)]^2$  is the reflectance and  $n$  the refractive index at the excitation wavelength,  $\lambda_{\text{exc}}$ . With these experimental data, the parameters  $\Theta = \theta/P\alpha L_{\text{eff}}$  were determined to the undoped ( $\Theta_{\text{undoped}}$ ) and Yb-doped ( $\Theta_{\text{doped}}$ ) samples. Here,  $L_{\text{eff}} = [1 - \exp(-\alpha L)]/\alpha$  needs to be used for high values of  $\alpha$ . By dividing  $\Theta_{\text{doped}}$  by  $\Theta_{\text{undoped}}$  the fraction of the absorbed energy converted into heat ( $\varphi$ ) is determined, which is related to  $\eta$  by:  $\Theta_{\text{doped}}/\Theta_{\text{undoped}} = \varphi = 1 - \eta(\lambda_{\text{exc}}/\lambda_{\text{em}})$ , with  $\langle \lambda_{\text{em}} \rangle$  being the average emission wavelength. Although it was possible to measure  $\theta/P$  for both undoped TL and TW samples, their absorption coefficient values could not be determined because the very low value at 950 nm. The experimental error is higher than the obtained value. To solve this problem we can use a thick sample to determine a more precise value to the relation  $P/P_0$ , or the TLS can be performed with excitation in a region where the absorption is higher, as in the visible region, since the sample must not present luminescence. The latter was recently used to determine  $\Theta$  values for the undoped

TL [24] and TW [7] glasses. By exciting them at 514 nm the obtained values were  $\Theta_{undoped}^{TL} = (26 \pm 1) \text{ W}^{-1}$  and  $\Theta_{undoped}^{TW} = (37 \pm 4) \text{ W}^{-1}$ . With these values it is possible to estimate the absorption coefficient at 950 nm, which are 0.056 and  $0.061 \text{ cm}^{-1}$  for the TL and TW, respectively. In fact, these low values are very difficult to be measured. This is the main difficulty in using the conventional TLS with a reference sample to measure the fluorescence quantum efficiency. By using our previous data for the reference undoped samples, the  $\eta$  values were determined and are listed in Table 1 as  $\eta_{ref}$ . A discussion on the concentration quenching and the obtained  $\eta_{ref}$  values will be done latter, after all the results are shown.

Following, the multiwavelength TLS was performed in the Yb-doped samples. In this procedure, the samples were excited at different energies between 928 and 970 nm, and the  $\Theta_{doped} = \theta / P\alpha L_{eff}$  values were obtained in function of the excitation wavelength. As mentioned before,  $\theta$  values were obtained for different excitation powers in order to find a better value to the ratio  $\theta/P$ . The product  $\alpha L_{eff}$  was measured for each excitation wavelength, by following the Beer's Law methodology described above. The  $\Theta_{doped}$  data for the doped Yb<sup>3+</sup>-doped TW glasses are shown in Fig. 3, which are similar to those obtained for the Yb<sup>3+</sup>-doped TL glass (not shown). The observed linear decrease in  $\Theta_{doped}$  with the excitation wavelength is expected since the fraction of the absorbed energy converted into heat also decrease. From a linear fit of the experimental data was possible to find the linear and angular coefficients, so that, by relation  $\Theta_{doped}(\lambda_{exc}) = \Theta_{undoped}[1 - \eta(\lambda_{exc}/\langle\lambda_{em}\rangle)]$ ,  $\eta$  can be determined for the doped glasses. The linear coefficient is used to characterize the thermo-optical parameters of the undoped sample. The linear coefficient is in fact  $\Theta_{undoped} = (1/\lambda_p K) ds/dT$ , in which  $\lambda_p$  is the probe wavelength,  $K$  is the thermal conductivity and  $ds/dT$  the temperature coefficient of the optical path length. From linear fit, the average values of the linear coefficient of TL and TW glasses were determined, providing  $\Theta_{undoped} = (36 \pm 6)$  and  $(55 \pm 9) \text{ W}^{-1}$ , respectively. These values are higher than those ones determined before by measuring the undoped samples. Our hypothesis to this discrepancy is that the angular coefficient in Fig. 3 is a very little parameter. Besides, as the linear coefficient is defined at  $\lambda_{exc} = 0$ , it is far from the excitation region, which can be considered very short. The consequence is that a small increase in  $\Theta_{doped}$  can be observed from  $\lambda_{exc} = 970$  to 928 nm, independently of the Yb concentration. This increase is

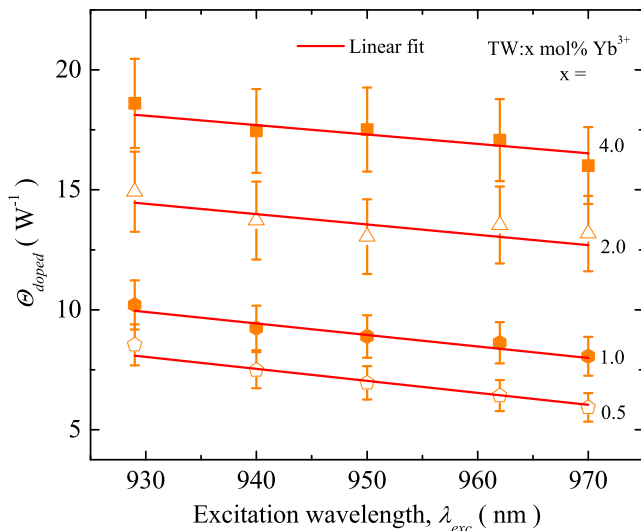


Fig. 3. Normalized thermal lens signal in function of the excitation wavelength for different Yb<sup>3+</sup> concentrations in TW glass.

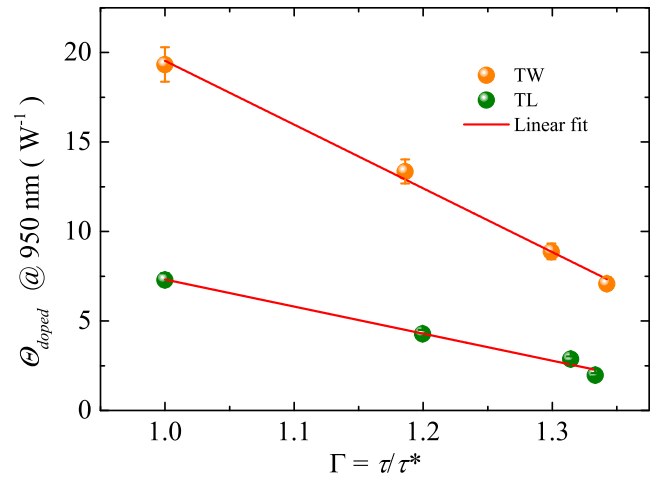


Fig. 4. Normalized thermal lens signal in function of the normalized lifetime for both TL and TW glasses.

related to the Yb<sup>3+</sup> quantum defect that is proportional to the heat created in the sample by the pump laser. This is an inconvenience to use this procedure in Yb-doped system. Anyway, in order to determine the absolute value for  $\eta$ , the angular coefficients obtained by the linear fit in Fig. 3 were divided by the linear one and multiplied by the average emission wavelengths obtained by the emission spectra in Fig. 1. The obtained  $\eta$  values for each Yb<sup>3+</sup> doped samples by using the multiwavelength TLS are also listed in Table 1 as  $\eta_{multi}$ . Although  $\Theta_{undoped}$  is different among the two methods described before, it can be noted that the obtained  $\eta_{ref}$  and  $\eta_{multi}$  values are equal if consider the experimental error. A complete discussion on the absolute value will be given latter.

Finally, the normalized lifetime TLS was used in our samples for determination of the fluorescence quantum yield,  $\eta_{norm}$ . For this purpose, the experimental luminescence lifetime,  $\tau$ , was firstly measured for each Yb-doped sample by exciting them at 920 nm. An exponential time dependence of the luminescence decay was observed for all of them, independent to the Yb concentration, and for both sample sets there are concentration quenching effect. So, the fluorescence quantum yield of the samples can be rewritten as  $\eta(N_t) = \eta^* \Gamma(N_t)$ , with  $\Gamma(N_t) = \tau/\tau^*$  being the experimental

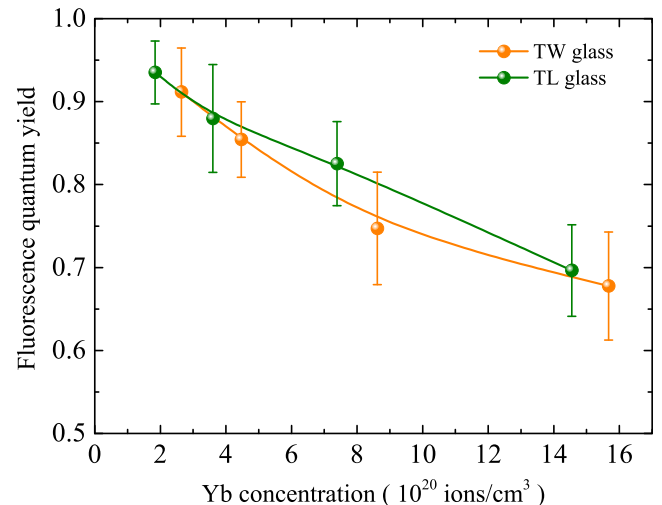


Fig. 5. Average fluorescence quantum yield for TL and TW glasses in function of the Yb concentration.





to represent the partial energy diagram of  $\text{Yb}^{3+}$ ,  $\text{Er}^{3+}$  and TL and TW hosts for our discussion. By the figure it is possible to note that when  $\text{Er}^{3+}$  is present into the host as impurity, there is a possibility of energy transfer between  $\text{Yb}^{3+}$  and  $\text{Er}^{3+}$ , so that the higher energy level of  $\text{Er}^{3+}$  can be promoted. In order to check whether  $\text{Er}^{3+}$  is an impurity in the system, 4.0 mol% of  $\text{Yb}^{3+}$  doped TL and TW glasses were excited to observe the  $\text{Er}^{3+}$  visible emission. In Fig. 6(b) the visible emission spectrum is plotted (solid line) for TL glass for excitation at 489 nm, which is characteristic of the  $\text{Er}^{3+}$  ion. When the TL glass was excited at 930 nm, similar visible emission (upconversion effect) was also observed (dot-dash line), indicating the energy transfer mechanism between  $\text{Yb}^{3+}$ – $\text{Er}^{3+}$ . Similar spectra were also obtained for TW glass, but the visible emission intensities are considerably lower (not shown). The reasons for this is that the ion–host interaction is more pronounced in TW than TL host, due to the overlap among the  $\text{Er}^{3+}$  emission levels and the TW host (see Fig. 6(a)). Finally, as hundreds of ppm of  $\text{OH}^-$  impurities are present in both glasses, as shown in Fig. 6(c), they can also contribute to the observed concentration quenching.

As mentioned,  $\Theta_{\text{undoped}}$  is related to the host intrinsic parameters, with  $K$  dependent on the thermal diffusivity ( $D$ ) of the sample by  $K = \rho CD$ , in which  $\rho$  is the volumetric density (see Table 1) and  $C$  is the specific heat of the sample [28]. Once  $D$  can also be determined during the TLS procedure, we investigated the obtained values for TW and TL glasses, which were  $(2.1 \pm 0.1)$  and  $(2.6 \pm 0.2) \times 10^{-3} \text{ cm}^2/\text{s}$ , respectively, independent of the Yb concentration and the used TLS methodology. The thermal diffusivity for TL glass agrees to the literature reported value [8]. This considerable difference ( $\sim 19\%$ ) among  $D$  values for the two sample sets, are from the same order of the difference obtained in the densities ( $\sim 17\%$ ), so that is reasonable to suppose that  $K$  is practically the same for all studied sample (see densities values in Table 1). With these considerations and using an average value for  $\langle \Theta_{\text{undoped}}^{\text{TW}} \rangle = 49 \text{ W}^{-1}$ ,  $ds/dT \sim 2.0 \times 10^{-5} \text{ K}^{-1}$  was estimated for TW glass, which is practically twice higher than the value for TL glass [24].

#### 4. Conclusions

Within the experimental limitation of each TLS procedure, it is possible to affirm that the fluorescence quantum yield for low ion concentration in both  $\text{Yb}^{3+}$ -doped tellurite hosts are high ( $>90\%$ ). The obtained values are higher than those reported for other tellurite glasses ( $\sim 80\%$ ). Although the studied  $\text{Yb}^{3+}$ -doped samples exhibit concentration quenching due to impurities,  $\text{OH}^-$  and ion–host interaction, its effect on the fluorescence quantum yield is not so strong, indicating that TL and TW tellurite glasses can be synthesized with  $\text{Yb}^{3+}$  concentration  $>1.6 \times 10^{21} \text{ ions/cm}^3$ . This is interesting for the use of the  $\text{Yb}^{3+}$  ion as activator in a co-doped tellurite system for application as spectral matching in Silicon solar cells.

#### Acknowledgments

The authors thank Coordenação de Aperfeiçoamento de Pessoal de Nível Superior, Conselho Nacional de Desenvolvimento Científico e Tecnológico, Fundação de Amparo à Pesquisa do Estado de São Paulo (FAPESP – 2013/19747-9) and Fundação de Apoio ao Desenvolvimento do Ensino, Ciência e Tecnologia do Estado de Mato Grosso do Sul (FUNDECT – 59/300.031/2015 and 23/200.735/2014) for financial support.

We dedicate this paper to Prof. Georges Boulon and would like to take this special occasion to express our gratitude and admiration to him. His important contribution towards a better understanding of several luminescence processes has impacted the

scientific life of many researches. Specially, his legacy to the better knowledge of the  $\text{Yb}^{3+}$  emission in several systems has benefited many researchers worldwide.

#### References

- [1] B.M. van der Ende, L. Aarts, A. Meijerink, Lanthanide ions as spectral converters for solar cells, *Phys. Chem. Chem. Phys.* 11 (2009) 11081–11095.
- [2] P. Vergeer, T.J.H. Vlugt, M.H.F. Kox, M.I. den Hertog, J.P.J.M. van der Eerden, A. Meijerink, Quantum cutting by cooperative energy transfer in  $\text{Yb}_x\text{Y}_{1-x}\text{PO}_4$ :  $\text{Tb}^{3+}$ , *Phys. Rev. B* 71 (2005) 014119.
- [3] X. Zou, H. Toratani, Evaluation of spectroscopic properties of  $\text{Yb}^{3+}$ -doped glasses, *Phys. Rev. B* 52 (1995) 15889–15897.
- [4] C. Jacinto, S.L. Oliveira, L.A.O. Nunes, T. Catunda, M.J.V. Bell, Thermal lens study of the  $\text{OH}^-$  influence on the fluorescence efficiency of  $\text{Yb}^{3+}$ -doped phosphate glasses, *Appl. Phys. Lett.* 86 (2005) 071911.
- [5] F.B. Costa, K. Yukimitu, L.A.O. Nunes, L.H.C. Andrade, S.M. Lima, J.C.S. Moraes, Characterization of  $\text{Nd}^{3+}$ -doped Tellurite glasses with low OH content, *Mater. Res.* 18 (2015) 2–7.
- [6] M.S. Figueiredo, F.A. Santos, K. Yukimitu, J.C.S. Moraes, J.R. Silva, M.L. Baesso, L.A.O. Nunes, L.H.C. Andrade, S.M. Lima, Luminescence quantum efficiency at  $1.5 \mu\text{m}$  of  $\text{Er}^{3+}$ -doped tellurite glass determined by thermal lens spectroscopy, *Opt. Mater.* 35 (2013) 2400–2404.
- [7] F.B. Costa, K. Yukimitu, L.A.O. Nunes, M.S. Figueiredo, L.H.C. Andrade, S.M. Lima, J.C.S. Moraes, Spectroscopic properties of  $\text{Nd}^{3+}$ -doped tungsten–tellurite glasses, *J. Phys. Chem. Solids* 88 (2016) 54–59.
- [8] M.S. Figueiredo, F.A. Santos, K. Yukimitu, J.C.S. Moraes, L.A.O. Nunes, L.H.C. Andrade, S.M. Lima, On observation of the downconversion mechanism in  $\text{Er}^{3+}/\text{Yb}^{3+}$  co-doped tellurite glass using thermal and optical parameters, *J. Lumin.* 157 (2015) 365–370.
- [9] R.A.H. El-Mallawany, *Tellurite Glasses Handbook: Physical Properties and Data*, second ed., CRC Press LLC, USA, 2011.
- [10] I. Jlassi, H. Elhouichet, M. Ferid, C. Barthou, Judd–Ofelt analysis and improvement of thermal and optical properties of tellurite glasses by adding  $\text{P}_2\text{O}_5$ , *J. Lumin.* 130 (2010) 2394–2401.
- [11] E.B. Intyushin, V.A. Novikov, Tungsten–tellurite glasses and thin films doped with rare-earth elements produced by radio frequency magnetron deposition, *Thin Solid Films* 516 (2008) 4194–4200.
- [12] C. Würth, M. Grabolle, J. Pauli, M. Spieles, U. Resch-Genger, Relative and absolute determination of fluorescence quantum yields of transparent samples, *Nat. Protoc.* 8 (2013) 1535–1550.
- [13] E.P. Tomasini, E. San Roman, S.E. Braslavsky, Validation of fluorescence quantum yields for light-scattering powdered samples by laser-induced optoacoustic spectroscopy, *Langmuir* 25 (2009) 5861–5868.
- [14] J. Olmsted, Calorimetric determinations of absolute fluorescence quantum yields, *J. Phys. Chem.* 83 (1979) 2581–2584.
- [15] C. Würth, M.G. González, R. Niessner, U. Panne, C. Haisch, U.R. Genger, Determination of the absolute fluorescence quantum yield of rhodamine 6G with optical and photoacoustic methods-providing the basis for fluorescence quantum yield standards, *Talanta* 90 (2012) 30–37.
- [16] M.L. Baesso, A.C. Bento, A.A. Andrade, J.A. Sampaio, E. Pecoraro, L.A.O. Nunes, T. Catunda, S. Gama, Absolute thermal lens method to determine fluorescence quantum efficiency and concentration quenching of solids, *Phys. Rev. B* 57 (1998) 10545–10549.
- [17] X. Feng, C. Qi, F. Lin, H. Hu, Tungsten–tellurite glass: a new candidate medium for  $\text{Yb}^{3+}$ -doping, *J. Non-Cryst. Solids* 256&257 (1999) 372–377.
- [18] S.M. Lima, A.A. Andrade, R. Lebullenger, A.C. Hernandez, T. Catunda, M.L. Baesso, Multiwavelength thermal lens determination of fluorescence quantum efficiency of solids: application to  $\text{Nd}^{3+}$ -doped fluoride glass, *Appl. Phys. Lett.* 78 (2001) 3220–3222.
- [19] C. Jacinto, S.L. Oliveira, L.A.O. Nunes, J.D. Myers, M.S. Myers, T. Catunda, Normalized-lifetime thermal-lens method for the determination of luminescence quantum efficiency and thermo-optical coefficients: application to  $\text{Nd}^{3+}$ -doped glasses, *Phys. Rev. B* 73 (2006) 125107.
- [20] J.C.S. Moraes, J.A. Nardi, S.M. Sidel, B.G. Mantovani, K. Yukimitu, V.C.S. Reynoso, L.F. Malmonge, N. Ghofraniha, G. Ruocco, L.H.C. Andrade, S.M. Lima, Relation among optical, thermal and thermo-optical properties and niobium concentration in tellurite glasses, *J. Non-Cryst. Solids* 356 (2010) 2146–2150.
- [21] D.E. McCumber, Einstein relations connecting broadband emission and absorption spectra, *Phys. Rev.* 136 (1964) A954–A957.
- [22] H. Yin, P. Deng, J. Zhang, F. Gan, Determination of emission cross section of  $\text{Yb}^{3+}$  in glasses by the reciprocity method, *Mater. Lett.* 30 (1997) 29–33.
- [23] J. Shen, R.D. Lowe, R.D. Snook, A model for cw laser induced mode-mismatched dual-beam thermal lens spectrometry, *Chem. Phys.* 165 (1992) 385–396.
- [24] S.M. Lima, W.F. Falco, E.S. Bannwart, L.H.C. Andrade, R.C. Oliveira, J.C.S. Moraes, K. Yukimitu, E.B. Araújo, E.A. Falcão, A. Steimacher, N.G.C. Astrath, A.C. Bento, A.N. Medina, M.L. Baesso, Thermo-optical characterization of tellurite glasses by thermal lens, thermal relaxation calorimetry and interferometric methods, *J. Non-Cryst. Solids* 352 (2006) 3603–3607.
- [25] L.R.P. Kassab, R.A. Kobayashi, M.J.V. Bell, A.P. Carmo, T. Catunda, Thermo-optical parameters of tellurite glasses doped with  $\text{Yb}^{3+}$ , *J. Phys. D Appl. Phys.* 40

- (2007) 4073–4077.
- [26] D.S. Sumida, T.Y. Fan, Effect of radiation trapping on fluorescence lifetime and emission cross section measurements in solid-state laser media, *Opt. Lett.* 19 (1994) 1343–1345.
- [27] P. Yang, P. Deng, Z. Yin, Concentration quenching in Yb:YAG, *J. Lumin.* 97 (2002) 51–54.
- [28] S.M. Lima, J.A. Sampaio, T. Catunda, A.C. Bento, L.C.M. Miranda, M.L. Baesso, Mode-mismatched thermal lens spectrometry for thermo-optical properties measurement in optical glasses: a review, *J. Non-Cryst. Solids* 273 (2000) 215–227.